JOURNAL OF GEOPHYSICAL RESEARCH, VOL. 115, D00H21, doi:10.1029/2009JD012389, 2010

Click Here for Full Article

AERONET, airborne HSRL, and CALIPSO aerosol retrievals compared and combined: A case study

Christopher J. McPherson,[1] John A. Reagan,[1] Joel Schafer,[2] David Giles,[2] Rich Ferrare,[3] John Hair,[3] and Chris Hostetler[3]

Received 30 April 2009; revised 13 November 2009; accepted 11 December 2009; published 30 April 2010.

[1] On 4 August 2007 a unique opportunity for the intercomparison of aerosol retrievals occurred as part of the Cloud-Aerosol Lidar and Infrared Pathfinder Satellite Observation (CALIPSO) and Twilight Zone (CATZ) campaign in the Washington, D. C., urban complex. During the course of the experiment, several Aerosol Robotic Network (AERONET) Cimel Sun photometers were deployed along the CALIPSO track, together with NASA Langley Research Center's airborne High Spectral Resolution Lidar (HSRL) instrument flying overhead. A series of daytime coincident measurements was made by the various instruments, permitting a number of important opportunities for the intercomparison of the various instrumental measurements of aerosols as well as evaluation of the Constrained Ratio Aerosol Model-fit (CRAM) technique for aerosol retrievals from elastic backscatter lidar. The results from the intercomparison are discussed as an illustrative case study in sensor combination and aerosol retrieval methodology.

Citation: McPherson, C. J., J. A. Reagan, J. Schafer, D. Giles, R. Ferrare, J. Hair, and C. Hostetler (2010), AERONET, airborne HSRL, and CALIPSO aerosol retrievals compared and combined: A case study, *J. Geophys. Res.*, *115*, D00H21, doi:10.1029/2009JD012389.

1. Introduction

[2] The Cloud-Aerosol Lidar and Infrared Pathfinder Satellite Observation (CALIPSO) daytime overpass of the Washington, D. C., urban complex on 4 August 2007 provided an excellent opportunity to measure an optically thick layer of urban/industrial aerosol just West of the city. CALIPSO, along with the NASA Langley Research Center's airborne High Spectral Resolution Lidar (HSRL) and Aerosol Robotic Network (AERONET) Cimel solar radiometers/Sun photometers all performed well, showing remarkable agreement in independent measurements/inferences of the 532 and 1064 nm aerosol optical depth (AOD), Ångström exponent, and the extinction-to-backscatter ratio S_a at 532 and 1064 nm. The Cimel instruments were operated throughout the day of the overpass, collecting data frequently enough to provide useful observations within minutes of the CALIPSO overpass as conditions were clear enough for direct solar viewing. The aerosol distribution was also sufficiently uniform to permit further sky-scanning measurements to be made. This paper concentrates on the intercomparison of results from these three classes of sensors, elaborating on the implications for the Constrained Ratio Aerosol Model-fit (CRAM) technique for aerosol retrieval, used in this case with CALIPSO data. The ground track for CALIPSO and the NASA B200 King Air aircraft on which the HSRL instrument was deployed, as well as the positioning of the Cimels is shown in Figure 1. The three Cimel sites addressed in this paper are the three shown as "x" marks at the southeast end of the track, directly west of Washington, D. C. The southernmost site is Ormond Middle School (38.856N, 77.455W), followed by Westfield High School (38.887N, 77.465W) and Sanders Elementary (39.038N, 77.510W).

2. Measurements

[3] The three instruments involved in these measurements were organized as part of the CALIPSO and Twilight Zone (CATZ) experiment, a series of nine such field campaigns taking place in Virginia and Maryland between 26 June and 29 August 2007.

2.1. CATZ and AERONET

[4] The CALIPSO and Twilight Zone (CATZ) experiment was a focused part of the larger AERONET mission of collecting large amounts of data relating to aerosol optical and radiative properties through a federated instrumentation network, directed under the auspices of the AERONET program insofar as the instrumentation and data processing methods used in the experiment were the same as those prescribed under the broader AERONET mission [*Holben et al.*, 1998].

[5] A principal objective of the campaign was the detailed investigation of the properties of particles inhabiting the "twilight zone" between aerosol and cloud layers, using joint inversions between the ground-based sky radiance measurements from Cimels and additional measurements from

[1]Department of Electrical and Computer Engineering, University of Arizona, Tucson, Arizona, USA.
[2]SSAI, NASA Goddard Space Flight Center, Greenbelt, Maryland, USA.
[3]NASA Langley Research Center, Hampton, Virginia, USA.

Copyright 2010 by the American Geophysical Union.
0148-0227/10/2009JD012389

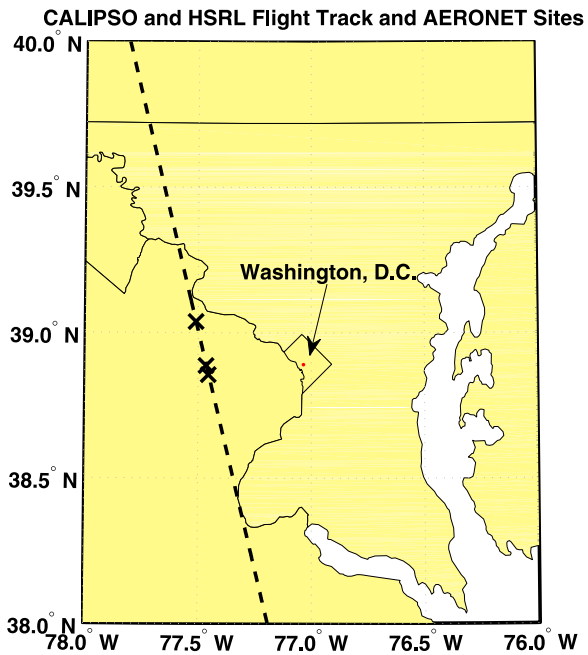

Figure 1. Map of Cloud-Aerosol Lidar and Infrared Pathfinder Satellite Observation (CALIPSO) and High Spectral Resolution Lidar (HSRL) flight tracks (4 August 2007 CALIPSO and Twilight Zone (CATZ) mission).

CALIPSO. Further, lidar (extinction-to-backscatter) ratio estimates were derived, using the method of *Dubovik and King* [2000] and *Dubovik et al.* [2006], from the AERONET almucantar products (to include single scattering albedo, refractive index and the phase function) to build a more comprehensive record of the microphysical properties characterizing these particles. Finally, the direct AOD measurements from the Cimel instruments were used to compare with those retrieved from CALIPSO in order to validate the aerosol retrieval methods. Data from the Cimel instruments were manually cloud-screened.

2.2. High Spectral Resolution Lidar

[6] The airborne High Spectral Resolution Lidar, unlike total backscatter lidars, uses a well-characterized, narrowband, molecular Iodine absorption filter to distinguish between aerosol and molecular scattering at 532 nm [*Hair et al.*, 2008]. The absorption properties of the filter are sufficient to eliminate the narrowband aerosol component from the backscattered signal, while leaving the Doppler-broadened molecular signal mostly intact. The result is a two-channel, polarization sensitive system at 532 nm, with one channel sensing the total backscatter and the other, which passes through the absorption filter, a purely molecular channel. The instrument is described as being self-calibrating at 532 nm, though an accurate atmospheric profile is needed in order to obtain the aerosol backscatter profile through a simple ratioing of the two channels. The atmospheric profiles for a particular mission may be obtained to a high degree of precision from nearby sonde measurements or from assimilated data. In addition, the aerosol extinction profile is obtained by taking the derivative of the aerosol transmittance term point-by-point and averaging vertically (300 m, or 10 range bins) to boost the signal-to-noise ratio (SNR). Thus, the aerosol backscatter and extinction profiles, and consequently, the extinction-to-backscatter ratio, are quite accurately known at 532 nm from the measurements made by HSRL [*Rogers et al.*, 2009].

[7] The airborne HSRL also employs a polarization sensitive, total backscatter lidar at 1064 nm. The calibration at 1064 nm is complicated by the fact that the aircraft flies at too low an altitude (~9 km) to routinely employ cirrus backscatter normalization to the 532 nm calibration [*Reagan et al.*, 2002]. Instead, calibration at 1064 nm relies on a transfer of the 532 nm calibration from nearly molecular scattering in clean-air regions. The systematic calibration error at 1064 nm is thus influenced by the presence of aerosols in the calibration region, the unknown scattering properties of which are thought to be sufficiently well bounded by models for the purposes of clean-air calibration.

2.3. CALIPSO and CRAM

[8] The Cloud-Aerosol Lidar with Orthogonal Polarization (CALIOP) is the principal instrument aboard the CALIPSO satellite [*Winker et al.*, 2009]. It is a standard dual-wavelength (532 and 1064 nm) total backscatter lidar with polarization sensitivity at 532 nm.

[9] The Constrained Ratio Aerosol Model-fit (CRAM) technique is a method of applying aerosol model parameters to the well-known problem of aerosol retrieval from multiple-wavelength elastic scatter lidar in order to significantly limit the amount of uncertainty in terms of the extinction-to-backscatter ratio and retrieved profiles of aerosol backscatter and extinction [*Reagan et al.*, 2004], particularly relative to current methods of S_a selection for retrieval of the CALIOP level 2 aerosol extinction products [*Omar et al.*, 2009]. (The current S_a selection algorithm used to generate the CALIOP level 2 aerosol product attempts to estimate S_a only to within ± 30%.) The CRAM technique relies upon a set of distinct aerosol models derived from global AERONET observations, which are thought to characterize various types of aerosols observed around the world [*Cattrall et al.*, 2005]. The models are defined around four principal aerosol scattering parameters, namely the extinction-to-backscatter ratio, S_a, at 532 nm and spectral ratios (532 to 1064 nm) of S_a, extinction and backscatter, which are closely related to microphysical and optical properties of the observed aerosols, e.g., complex refractive index and size distribution. By assuming S_a at the two wavelengths consistent with each model, corresponding profiles of aerosol extinction and backscatter at both wavelengths are then retrieved from the data through the Fernald retrieval relation [*Fernald et al.*, 1972; *Fernald*, 1984], yielding spectral ratios of aerosol backscatter and extinction to compare with the CRAM models. In general, three S_a values at 532 nm, representing the mean and ± standard deviations of a particular model are tested (along with the corresponding S_a values at 1064 nm given by the spectral ratio of S_a indicated by the model). The spectral ratios of extinction and backscatter retrieved from assuming these values are compared against the corresponding model "window," representing the ± standard deviation values of each corresponding spectral ratio parameter in the model. Normally, a model choice is considered acceptable if two pairs (out of three) of the retrieved spectral ratio parameters fall within the predicted "window." The particular S_a pair most closely

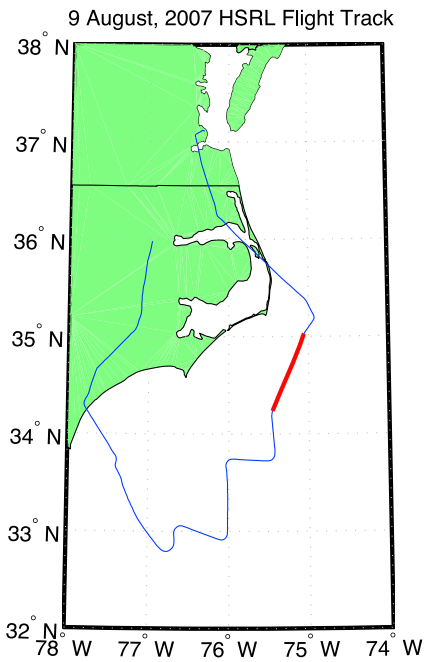

Figure 2. Map of HSRL flight track (9 August 2007).

matching the data is then selected on the basis of its minimization of a least squares performance function of the form

$$Q = \left(\frac{R_\beta^r - R_\beta^m}{R_\beta^m}\right)^2 + \left(\frac{R_\sigma^r - R_\sigma^m}{R_\sigma^m}\right)^2, \quad (1)$$

where R_β^r and R_σ^r represent the spectral ratios of aerosol backscatter and extinction, respectively, retrieved from the data according to the S_a pair assumed, and where R_β^m and R_σ^m represent the spectral values of backscatter and extinction, respectively, predicted by the associated model. The result of the analysis is a value of S_a at each wavelength together with retrieved aerosol backscatter and extinction profiles consistent with the one CRAM model determined from the performance function to be most closely aligned (in the sense of intrinsic aerosol properties) with the data. The CRAM technique is thus an appropriate retrieval method through which model constraints may be incorporated into the solution in a way that reduces the amount of uncertainty relative to alternate solutions that do not benefit from the added information of aerosol models in the context of dual-wavelength lidar information.

2.4. CRAM Applied to Data From HSRL

[10] Using dual-wavelength attenuated backscatter data from the NASA Langley Airborne HSRL, the CRAM method can be applied and the results at 532 nm validated against the aerosol extinction and backscatter as measured directly by the instrument. Validation and refinement of CRAM and its aerosol models through exploitation of the already vast and growing HSRL data set are ongoing topics of research.

[11] To illustrate, an HSRL flight from 9 August 2007 is presented, the flight track for which is shown in Figure 2. During the portion of the flight outlined in red, a high-AOD layer is overflown off Cape Hatteras along the North Carolina coast. The 532 and 1064 nm attenuated backscatter profiles for the segment are shown in Figure 3. From these, various retrievals are made using different pairings of the 532 and 1064 nm S_a consistent with each of the CRAM models. The spectral ratios of extinction and backscatter retrieved from each pair are then compared against what is predicted by each corresponding model to evaluate fitness of the retrieval to each model assumed. The comparison is made via a spatial mean of these ratios.

[12] The performance function of equation (1) is minimized for the aerosol model associated with biomass burning, with a

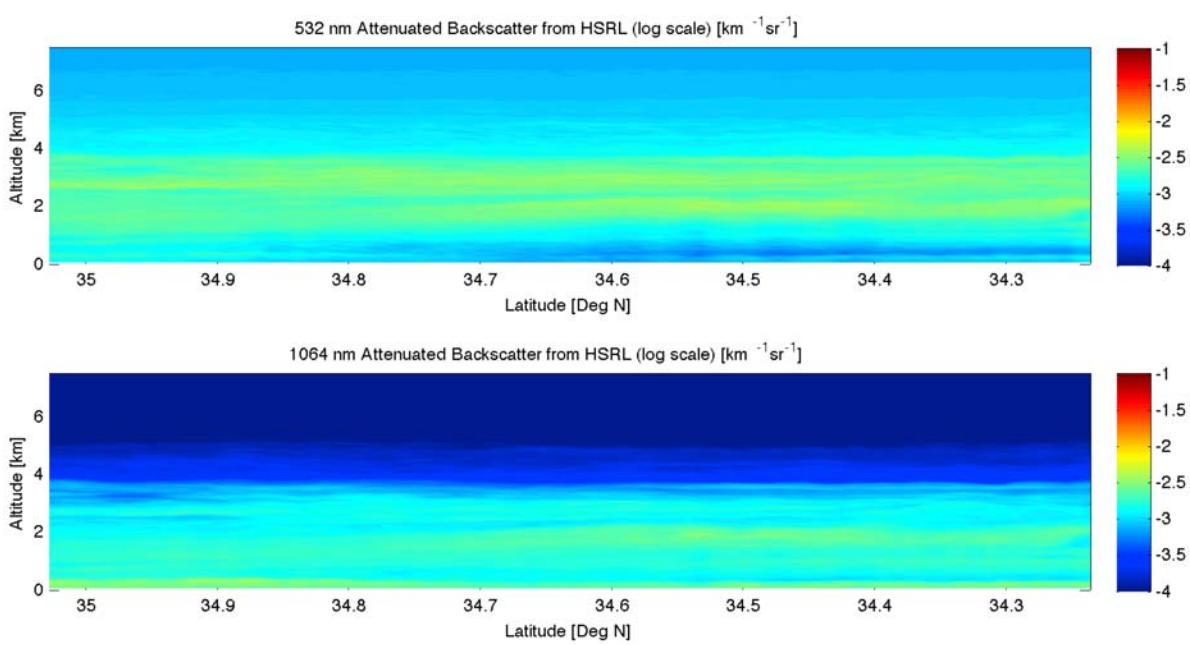

Figure 3. The 532 and 1064 nm attenuated backscatter profiles from HSRL from which aerosol retrievals are made via Constrained Ratio Aerosol Model-fit (CRAM).

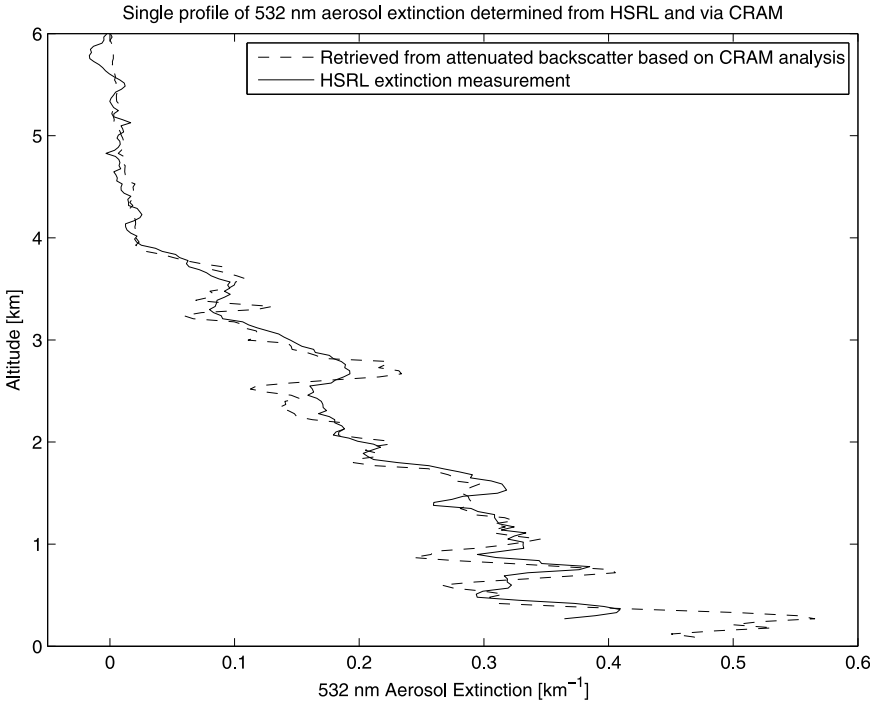

Figure 4. The 532 nm aerosol extinction as measured by HSRL and retrieved from attenuated backscatter via CRAM.

532 nm S_a of 68 sr. This compares well with the 532 nm S_a measured by the HSRL, having a spatial mean of about 71 sr. Predictably, a single extinction profile retrieval from the attenuated backscatter data based on the CRAM determined S_a at 532 nm compares very well with the measured extinction profile, as demonstrated in Figure 4. Small differences between the CRAM retrieval and the HSRL extinction are primarily due to spatial fluctuations in the true 532 nm S_a, as the value of S_a determined from CRAM is indeed very close to the true spatial mean. Differences in the overall AOD depend on where these fluctuations occur. Differences between the assumed S_a in areas of higher aerosol loading naturally have a larger effect on AOD than if they occur in areas of lower aerosol loading. On the whole however, the CRAM technique is a very reasonable approach, one which makes optimal use of the available dual-wavelength information in the context of aerosol models.

2.5. Summary of Data Products

[13] In order to give more meaning to the results to be presented and to clarify their significance, the various data products from the three sensors are classified as either primary or secondary. We describe a primary data product as one which is the result of a direct instrumental measurement by one of the sensors, subject only to the calibration uncertainty of the instrument itself. A secondary data product is one which has been derived from a primary data product through the application of some formulaic retrieval strategy or inversion methodology, typically involving particular assumptions or constraints with systematic uncertainties which may be difficult to evaluate, but which are nonetheless reasonable.

[14] For the Cimel products, we classify the spectral AOD and Ångström exponents as primary data products and the aerosol phase function and single scattering albedo (from which S_a may be determined) as secondary products derived from inversions [*Dubovik and King*, 2000; *Dubovik et al.*, 2006], applied to the almucantar scans made by the instrument. For HSRL, the 532 nm aerosol backscatter and extinction (and the extinction-to-backscatter ratio S_a at 532 nm) are all primary products, as they are all directly measured quantities. For CALIPSO, primary products include the lidar attenuated backscatter at 532 and 1064 nm as well as depolarization at 532 nm. The secondary products, aerosol extinction, backscatter, and the lidar ratio (S_a) at 532 and 1064 nm are available via dual-wavelength retrievals from the CRAM technique.

3. Results

[15] Overall, and especially in consideration of the increased noise levels experienced by CALIPSO during the daytime, agreement between all sensors was excellent in terms of both primary and secondary products. CRAM retrievals yielded results consistent with the high end of 532 nm S_a values expected for the urban/industrial (U/I) aerosol CRAM model, agreeing fairly closely with that measured/inferred by HSRL and the Cimel instruments. Shown in Figure 5 is a quicklook image illustrating (Figure 5, top) 532 nm aerosol extinction coefficients as measured by HSRL and (Figure 5, bottom) the 532 nm aerosol extinction coefficients as determined from CALIOP based on CRAM analysis. The red vertical bars in Figures 5 (top) and 5 (bottom) indicate the along-track position of the three Cimel sites, shown as "x" marks in Figure 1. Figure 5 (bottom), featuring the CALIOP data, is shown with 40 km horizontal "moving window" averaging (arising from preprocessing in the attenuated backscatter domain), necessary to increase the effective

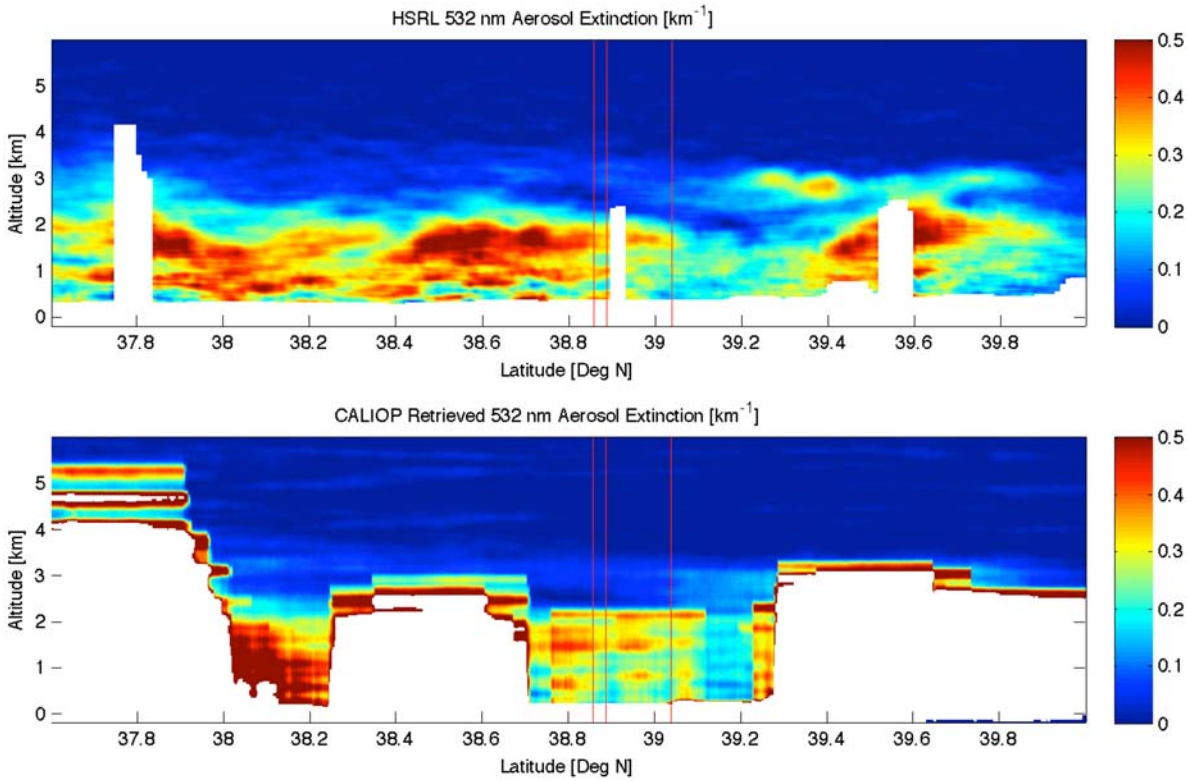

Figure 5. The 532 nm aerosol extinction from (top) HSRL and (bottom) Cloud-Aerosol Lidar with Orthogonal Polarization (CALIOP).

SNR for the daytime data. The HSRL data in Figure 5 (top) is averaged for one minute horizontally (~6 km) and vertically over 10 range bins (300 m). It is clear from Figure 5 that the agreement in aerosol extinction between CALIOP and HSRL is, visually, quite close in the vicinity of the Cimel sites. The large regions of the Figure 5 (bottom) showing no data are regions in which the retrieval solution is not valid, i.e., negative extinction or otherwise unreasonable/unstable solutions. Areas of cloud contamination or regions in which the aerosol properties no longer match those inferred from CRAM can easily give rise to this condition. We note, however, that any particular CRAM solution should only be considered valid in the region of aerosol subjected to the constraints of the method, in this case restricted to the neighborhood of the Cimel sites (~21 km). The surrounding region is shown more for the purpose of illustrating some broader spatial context relative to the HSRL measurements.

[16] Some difference in the 532 nm extinction is evident between the locations of the three Cimel sites, which is attributable to the combination of some real aerosol spatial variation, the smearing effect of the 40 km running average, and the potential inclusion in the average of some spotty clouds that are evident both in the HSRL aerosol backscatter product and in some of the Cimel measurements. A ~33 min temporal difference between HSRL and CALIPSO overpasses of the Cimel sites may also be meaningful, but is not considered a significant factor in our analysis. In general, this visual difference in extinction is not significant in consideration of the reduced SNR of CALIOP during the day. Substantial averaging (40 km) of the attenuated backscatter signal was necessary to facilitate a meaningful CRAM retrieval, which very likely contributed to the observed differences to some degree. The spectral ratio parameters retrieved from CRAM are shown in Figures 6 and 7, together with their corresponding model "windows" for the CRAM U/I model.

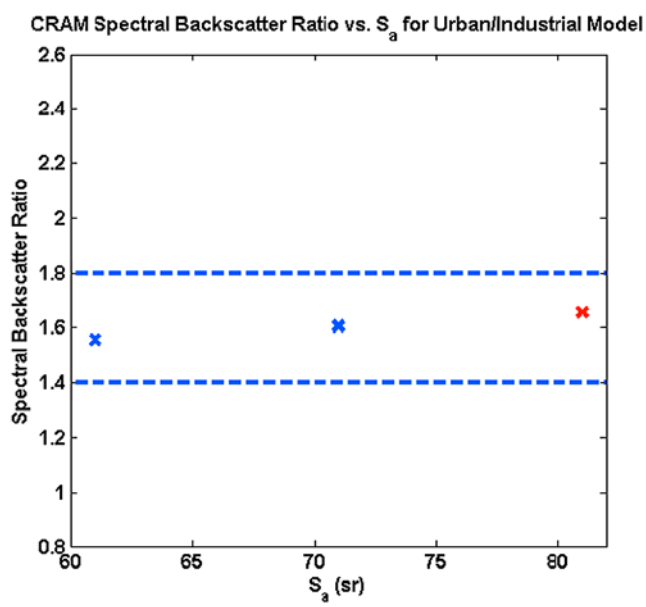

Figure 6. CRAM solutions for the spectral ratio of aerosol backscatter with the urban/industrial model window; "x" marks indicate mean 532 nm S_a and ± standard deviation solutions.

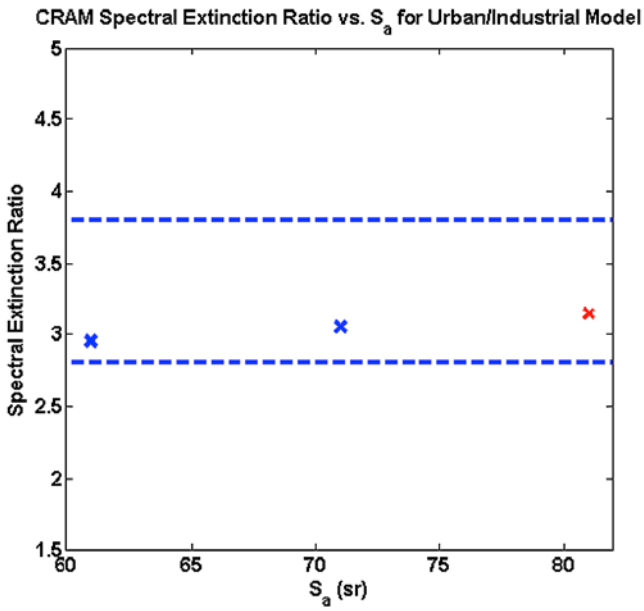

Figure 7. CRAM solutions for the spectral ratio of aerosol extinction with the urban/industrial model window; "x" marks indicate mean 532 nm S_a and ± standard deviation solutions.

The retrieved parameters come from a spatial average (bound roughly by the first and third Cimel locations along track) of the retrieved aerosol extinction and backscatter at 532 and 1064 nm based on the CRAM U/I model, using the mean and ± standard deviation values of S_a at 532 nm. The + standard deviation value of S_a at 532 nm (81), indicated by the red "x" mark in Figures 6 and 7, was selected for the retrieval based on its minimization of the least squares performance function of equation (1). A single 532 nm extinction profile was generated by taking an ensemble average of the CRAM/CALIOP retrieved extinction data over the area encompassed by the Cimel sites (~21 km). Doing so helps to ensure that any natural spatial inhomogeneity in the scattering properties of the aerosols in this region does not substantially affect the results in terms of the computed regional AOD. The HSRL

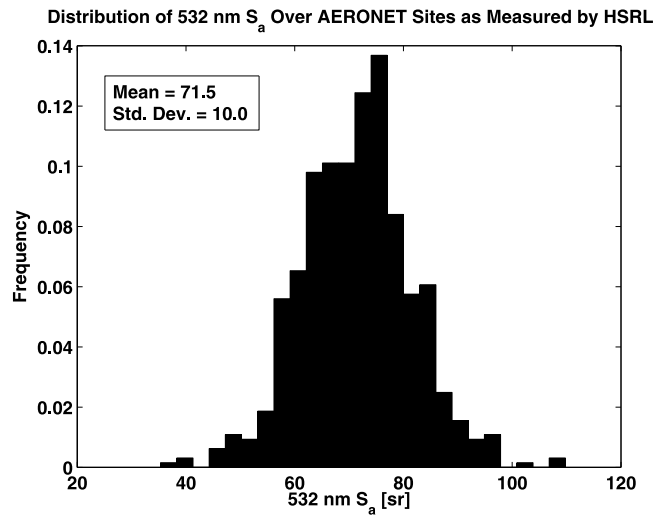

Figure 9. Spatial distribution of 532 nm S_a over the AERONET sites, measured by HSRL.

measured 532 nm S_a, as shown in Figure 8, when compared spatially with the same region, yields an average (averaged both vertically and horizontally) of 71.5 sr with a standard deviation of 10 sr, as illustrated in Figure 9. This is practically identical to the range predicted by the CRAM U/I model, which has a mean of 71 sr and standard deviation of 10 sr. Although the value determined from CALIOP data according to the performance function (81 sr) is somewhat higher than the mean measured by HSRL (71.5 sr), the value is still consistent with the U/I model, i.e., within the range of uncertainty of S_a at 532 nm.

[17] The 532 nm S_a computed from the Cimel inversions is in the neighborhood of 88 sr. For lack of a more precise systematic uncertainty estimate for this inversion, we place a ± 15% uncertainty on this value, consistent with the typical uncertainty associated with 532 nm S_a in the CRAM aerosol models [*Cattrall et al.*, 2005], leading to a value of 88 ± 13.2 sr. A similar ± 15% uncertainty was assumed for the Cimel 1064 nm S_a determination, for a value of ~40.5 ± 6.1 sr. This compares well with the CRAM U/I model S_a value at

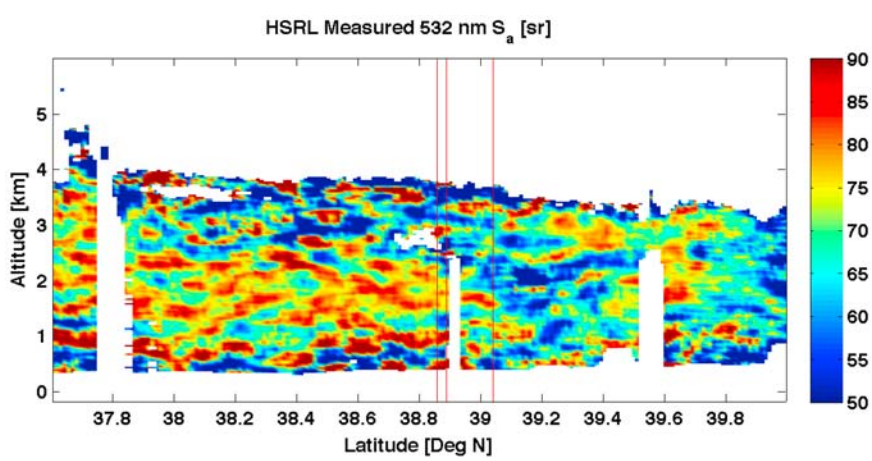

Figure 8. HSRL measured 532 nm S_a in the neighborhood of Aerosol Robotic Network (AERONET) sites.

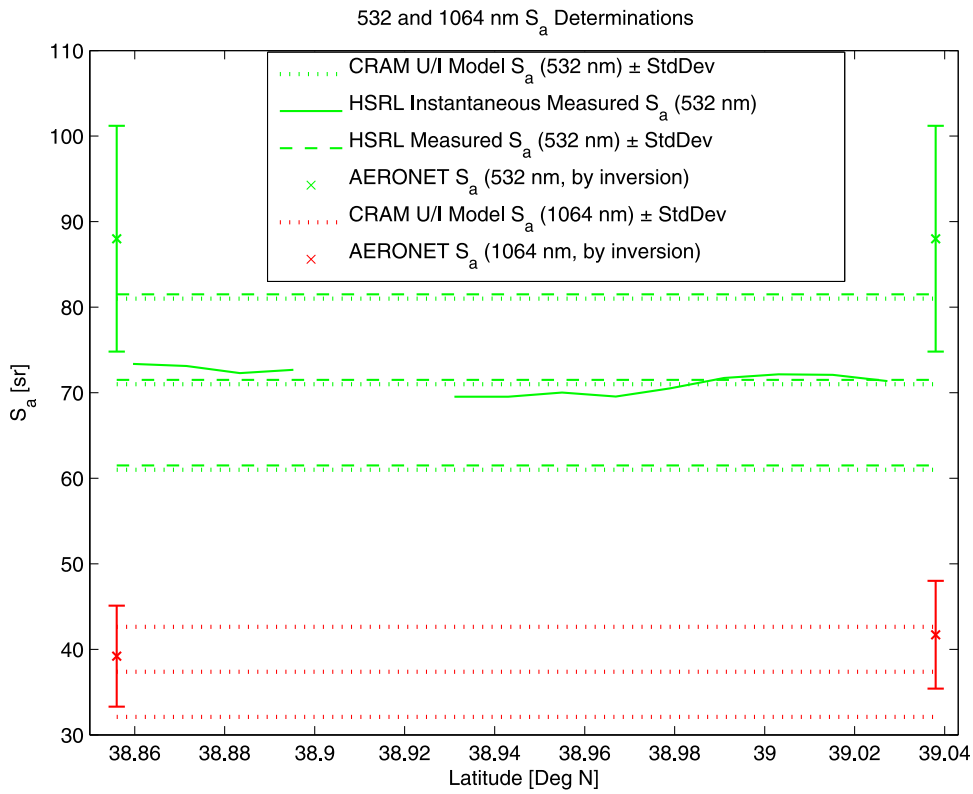

Figure 10. Summary of 532 and 1064 nm S_a determinations, from AERONET inferences from almucantar scan inversions, HSRL direct measurements at 532 nm, and CALIOP/CRAM inferences based on the U/I aerosol model.

1064 nm of 37.4 ± 5.3 sr. Determinations of the S_a values were available from the Cimel sites at Ormand and Sanders only, as Westfield experienced cloud cover which prevented meaningful almucantar inversions. A summary of the different instrumental determinations/inferences of S_a is presented in Figure 10.

[18] The agreement between the various S_a determinations is generally good. Perhaps more significantly than the three absolute 532 nm S_a determinations, the 532 nm aerosol extinction profile and optical depth estimated from CALIOP were found to be remarkably close to that measured by HSRL over the same region of spatial averaging. Additional 300 m vertical smoothing was applied to the CALIOP data to match that present in the aerosol extinction profiles of HSRL to produce as comparable a result as possible between the two instruments. Shown in Figure 11 is the intercomparison of the retrieved 532 nm aerosol extinction profile retrieved from CALIOP (dashed) using CRAM analysis (i.e., from the minimum Q 532 nm $S_a = 81$) set against the profile measured by HSRL (solid). This profile represents a spatial average over all of the Cimel sites to compensate for the low SNR achieved by CALIOP during the daytime. In addition, since the aerosol extinction product computed from the HSRL data involves a point-by-point derivative of the aerosol transmittance, a 300m vertical moving average is taken to boost SNR. This averaging results in a certain amount of lost signal near the ground, which must be accounted for in order to make an accurate and faithful estimate of AOD. The HSRL extinction data presented here has been extended to ground by taking the aerosol backscatter product (which is not averaged in the same way, and which does extend to the ground) and multiplying by the last available measured value of S_a near the ground for each vertical profile. The result in the integrated product (AOD) at 532 nm is 0.645 ± 0.097 and 0.642 ± 0.012 for CALIOP and HSRL, respectively.

[19] For the purposes of comparison, the CALIPSO provisional level 2 aerosol extinction product is also shown in Figure 11 (dotted). Since the CALIPSO level 2 data are presently only available in 40 km "chunks," it is impossible to subset in such a way as to achieve appropriate overlap in the region of the Cimel instruments, as has been done with HSRL and the CALIOP/CRAM retrievals (which come from the calibrated level 1 attenuated backscatter product). Nevertheless, the level 2 data presented here come from the profile closest to the spatial interval of interest. As is evident Figure 11, the level 2 algorithm fails to account for a substantial amount of aerosol below 1.45 km. This profile corresponds to an integrated AOD of 0.321, in error by approximately 50%. We note that these data are merely provisional, and that the level 2 algorithms are still very much in an experimental phase of development. In general however, it is the case that focused analysis of a particular region, of the sort presented in this paper, will almost always outperform algorithmic analysis whose purpose is to provide a "best guess" across all data in a computationally efficient manner.

[20] The uncertainty in the retrieved aerosol extinction from CALIPSO is on the order of the uncertainty in S_a, and the absolute S_a uncertainty may be treated as the dominant factor in its estimation. Other results have shown that the uncertainty in the retrieval is typically dominated by the un-

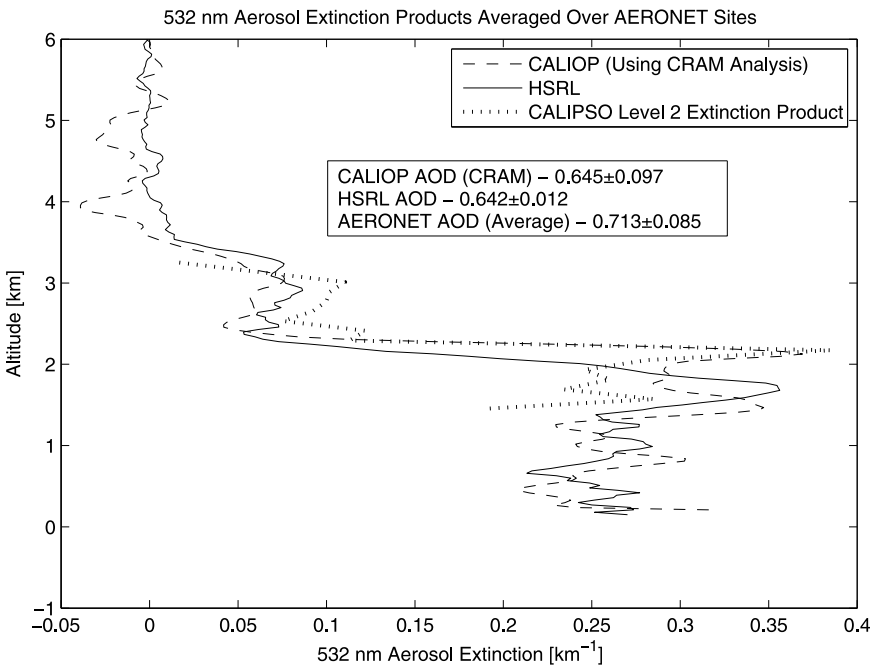

Figure 11. Aerosol extinction retrievals from HSRL and CALIOP, averaged over the area of the AERONET sites.

certainty in S_a, and is reasonably approximated by this value. Systematic uncertainty (arising from uncertainty in S_a) associated with aerosol properties retrieved from elastic scatter lidar has been studied elsewhere [*Sasano et al.*, 1985; *Braun*, 1985]. In particular, the uncertainty in retrieved AOD $\Delta\tau$ arising from some known S_a uncertainty ΔS_a can be described by

$$\Delta\tau = \frac{\exp[2\tau] - 1}{2}\frac{\Delta S_a}{S_a} \tag{2}$$

[21] Thus, the value of ± 0.097 for the CRAM retrieval corresponds to an uncertainty of ± 15%, similar to the uncertainty placed on S_a across the various aerosol models. The uncertainty in the HSRL AOD was estimated from the RMS fluctuation of the aerosol extinction product in a sample of clean air, and extended over the range of the AOD integration. The results, in terms of 532 and 1064 nm AOD are summarized in Figure 12 together with the AOD measurements made by the Cimel instruments. The AOD at each Cimel site is an average of AOD measurements made at 3 min intervals over a ± 15 min time window centered on the CALIPSO overpass, and the ± standard deviation bars given with each AOD reflect the combined effects of temporal variations over the averaging period and estimated instrument uncertainty. As the AERONET cloud-screening algorithm is not set up to support the 3 min sampling interval used during this experiment, the Cimel data were manually cloud-screened by restricting the temporal AOD variation across the entire overpass duration to within one standard deviation of the mean, thereby neglecting any very high AOD measurements which would result from clouds. This was done with the knowledge that there were many observations near the time of overpass in which clouds did not obstruct the instruments' view of the Sun. The AODs have also been scaled from the closest Cimel wavelength to the CALIOP wavelength (520nm to 532 nm and 1020 to 1064 nm) using the mean multiwavelength Ångström exponent computed from the Cimel spectral AOD observations. The average 532 nm AOD for the three Cimel sites is 0.713 ± 0.085 (listed in Figure 11) which, although slightly higher, compares very well with CALIOP and HSRL spatially averaged 532 nm AODs already cited in connection with the extinction profiles given in Figure 11. AOD at 1064 nm also compared very well between CALIOP and the Cimel instruments. Average 1064 nm AOD over the Cimel sites as computed from CALIOP/CRAM analysis was 0.193 ± 0.029, compared with 0.196 ± 0.035 computed from an average of data from the three Cimel instruments.

[22] We also note excellent agreement between the Ångström exponents computed from the Cimel observations relative to that predicted by the CRAM U/I model. Given our 550 to 1020 nm extinction ratio parameterization from the CRAM U/I model of 3.3 ± 0.5, we arrive at a modeled Ångström exponent of ~1.93 ± 0.25. Mean Ångström exponent values from the Cimel observations at the three sites are shown in Figure 13 together with the range of values predicted by the CRAM U/I aerosol model. The mean for the three Cimel sites is 1.88 ± 0.1, which is quite close to the mean U/I model value of 1.93 ± 0.25 (Figure 13).

4. Discussion and Conclusions

[23] Through analysis of coincident CALIPSO, airborne HSRL and AERONET (Cimel) data taken during the CATZ-F campaign of 4 August 2007, we have demonstrated excellent agreement between both primary and secondary aerosol products of the various sensors, including CRAM retrievals from the CALIPSO data. Furthermore, the analysis

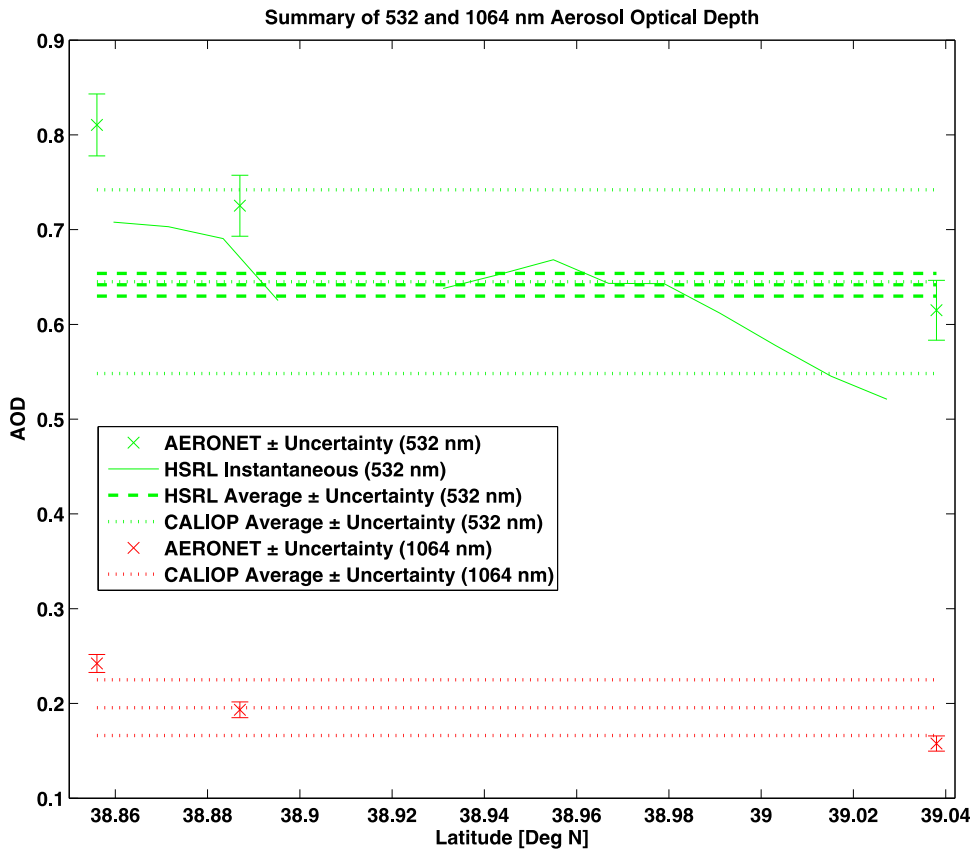

Figure 12. Summary of 532 and 1064 nm aerosol optical depth (AOD) retrievals/observations from the various sensors, from AERONET measurements (532 nm AOD estimated from 550 nm channel and 1064 nm AOD from 1020 nm channel using mean Ångström exponent), HSRL integrated extinction product at 532 nm, and CALIOP/CRAM aerosol retrievals at 532 and 1064 nm.

serves as a clear illustration of the effectiveness of the CRAM retrieval methodology as a means to fully exploit dual-wavelength elastic scatter lidar information to accurately retrieve key optical parameters of observed aerosols, particularly the aerosol extinction and backscatter profiles at both wavelengths.

[24] In particular, the agreement in aerosol optical depth results between the HSRL and CRAM processed CALIOP data are exceptional. That a secondary product from CALIOP's elastic scatter lidar would compare so favorably with the same primary measurement from HSRL is remarkable, especially in consideration of the background noise present during the day affecting both sensors. We attribute the small difference between CRAM/CALIOP and HSRL AODs and those determined by the Cimel instruments to the fact that the Cimel observes the full atmosphere above HSRL or, in the case of CALIOP, above the point at which any upper tropospheric or stratospheric aerosols may be lost in the noise. In any event, we do not make an attempt through CRAM to characterize these aerosols for the purposes of a retrieval, and so the likelihood is that any estimate of the AOD from either HSRL or CALIOP will invariably neglect some small amount of aerosol measurable by the Cimel instruments [*Rogers et al.*, 2009].

[25] Furthermore, CRAM, as we have implemented it, does not attempt to descend into finer granularity of S_a than the uncertainty spread implied by the models, despite the particular choice of S_a consistent with the minimum value of the performance function. Additionally, some minor differences in calibration may also affect the value determined by CRAM based on CALIOP data. Preliminary analysis has shown that nominal uncertainty associated with CALIOP calibration is not sufficient to push a normally valid solution out of the model "window" in terms of the retrieved aerosol extinction or backscatter spectral ratios. Naturally, since CRAM is based upon analysis of spectral ratios, there is a certain amount of insensitivity of the technique to calibration uncertainty at 532 nm since the 1064 nm channel is always calibrated relative to the 532 nm channel; that is, shift in the calibration at 532 nm drives a proportional shift at 1064 nm, the uncertainty of which is mitigated to some degree by virtue of dealing with spectral ratios. While gross miscalibration at 1064 nm (and, to a lesser extent, at 532 nm) certainly has the potential to upset CRAM, and while newer estimates of CALIOP calibration uncertainty [*Lee et al.*, 2008; *Powell et al.*, 2008] should motivate future study vis-à-vis its effects on the technique, we do not make an attempt here to account for hypothetically pathological cases, particularly in consideration of the consistency of our results. To the extent that CRAM delivers a valid solution as described in section 2.3, the dual-wavelength information in the data has been maximally exploited within the framework of the technique. Conse-

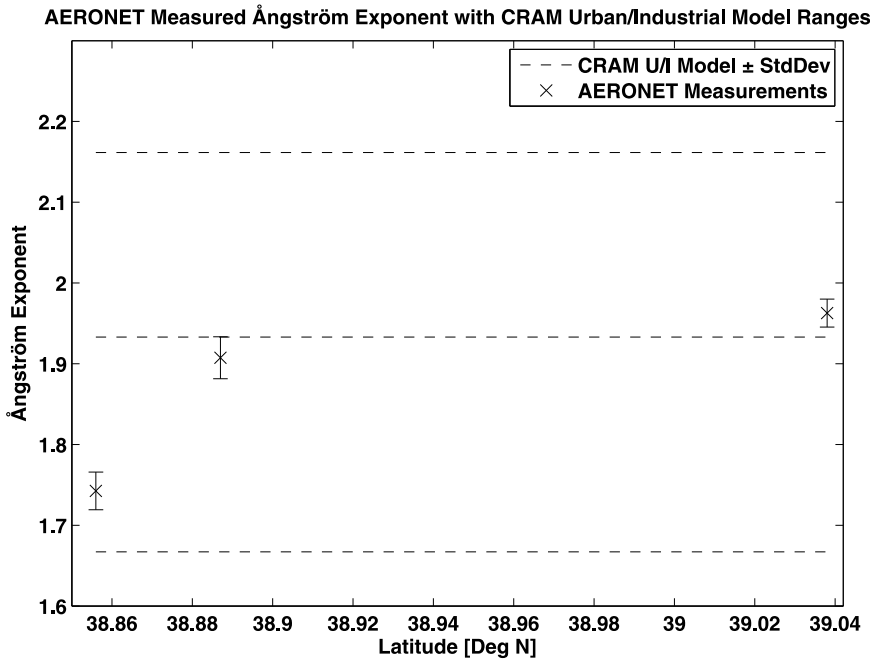

Figure 13. Cimel measurements of the Ångström exponent, against the CRAM urban/industrial model values.

quently, it is important to distinguish this technique from what might more accurately be called an inversion, where the intentional claim is that a solution for S_a can be analytically retrieved subject to some systematic uncertainty which is in general bound by that of the instrument.

[26] Further investigation is needed in the form of additional case studies with coincident observations of other aerosol types by multiple sensors, in particular CALIPSO and HSRL, to expand on this work and to further confirm the CRAM methodology as a reliable solution. It is hoped that as the method and, as importantly, the aerosol models used in the technique are developed, some degree of improvement can be made on the 30% uncertainty with which S_a is currently estimated for the CALIOP level 2 aerosol product. Work is in progress to confirm and, as needed, modify the CRAM aerosol models through analysis of HSRL observations of various classes of aerosol. Some success in this regard has already been achieved [*McPherson and Reagan*, 2010], in modifying the original CRAM Saharan Dust model through the use of both statistical assessments and an Enhanced CRAM (E-CRAM) solution approach that may be employed when added information about the CRAM aerosol parameters is available at one wavelength (e.g., as provided by HSRL observations).

[27] **Acknowledgments.** The authors wish to acknowledge the AERONET team for providing instrument calibration, field measurements, and data processing. This work was supported under the NASA Graduate Student Researchers Program Fellowship through contract NNX07AM11H, as well as under NASA contract NASA1-99102.

References

Braun, C. (1985), General formula for the errors in aerosol properties determined from lidar measurements at a single wavelength, *Appl. Opt.*, *24*(7), 925–927, doi:10.1364/AO.24.000925.

Cattrall, C., J. Reagan, K. Thome, and O. Dubovik (2005), Variability of aerosol and spectral lidar and backscatter and extinction ratios of key aerosol types derived from selected aerosol robotic network locations, *J. Geophys. Res.*, *110*, D10S11, doi:10.1029/2004JD005124.

Dubovik, O., and M. King (2000), A flexible inversion algorithm for retrieval of aerosol optical properties from Sun and sky radiance measurements, *J. Geophys. Res.*, *105*(D16), 20,673–20,696, doi:10.1029/2000JD900282.

Dubovik, O., et al. (2006), Application of spheroid models to account for aerosol particle nonsphericity in remote sensing of desert dust, *J. Geophys. Res.*, *111*, D11208, doi:10.1029/2005JD006619.

Fernald, F. G. (1984), Analysis of atmospheric lidar observations: Some comments, *Appl. Opt.*, *23*(5), 652–653, doi:10.1364/AO.23.000652.

Fernald, F. G., B. M. Herman, and J. A. Reagan (1972), Determination of aerosol height distributions by lidar, *J. Appl. Meteorol.*, *11*(3), 482–489, doi:10.1175/1520-0450(1972)011<0482:DOAHDB>2.0.CO;2.

Hair, J. W., et al. (2008), Airborne High Spectral Resolution Lidar for profiling aerosol optical properties, *Appl. Opt.*, *47*(36), 6734–6752, doi:10.1364/AO.47.006734.

Holben, B. N., et al. (1998), AERONET: A federated instrument network and data archive for aerosol characterization, *Remote Sens. Environ.*, *66*(1), 1–16, doi:10.1016/S0034-4257(98)00031-5.

Lee, K. P., M. Vaughan, Z. Liu, W. Hunt, and K. Powell (2008), Revised calibration strategy for the CALIOP 532 nm channel: Part I. Nighttime, paper presented at 24th International Laser Radar Conference, Lockheed Martin, Boulder, Colo., 23–27 June.

McPherson, C. J., and J. A. Reagan (2010), Analysis of optical properties of Saharan dust derived from dual-wavelength aerosol retrievals from CALIPSO Observations, *Geosci. Remote Sens. Lett.*, *7*, 98–102, doi:10.1109/LGRS.2009.2021677.

Omar, A. H., et al. (2009), The CALIPSO automated aerosol classification and lidar ratio selection algorithm, *J. Atmos. Oceanic Technol.*, *26*, 1994–2014, doi:10.1175/2009JTECHA1231.1.

Powell, K. A., M. A. Vaughan, R. Kuehn, W. H. Hunt, and K. P. Lee (2008), Revised calibration strategy for the CALIOP 532 nm channel: Part II. Daytime, paper presented at 24th International Laser Radar Conference, Lockheed Martin, Boulder, Colo., 23–27 June.

Reagan, J. A., X. Wang, and M. T. Osborn (2002), Spaceborne lidar calibration from cirrus and molecular backscatter returns, *IEEE Trans. Geosci. Remote Sens.*, *40*(10), 2285–2290, doi:10.1109/TGRS.2002.802464.

Reagan, J. A., X. Wang, C. Cattrall, and K. Thome (2004), Spaceborne lidar aerosol retrieval approaches based on aerosol model constraints, in *2004 IEEE International Geoscience and Remote Sensing Symposium Proceedings. IGARSS 2004*, pp. 1940–1943, IEEE, Piscataway, N. J., doi:10.1109/IGARSS.2004.1370723.

Rogers, R. R., et al. (2009), NASA LaRC airborne High Spectral Resolution Lidar aerosol measurements during MILAGRO: Observations and validation, *Atmos. Chem. Phys.*, *9*(14), 4811–4826.

Sasano, Y., E. V. Browell, and S. Ismail (1985), Error caused by using a constant extinction/backscattering ratio in the lidar solution, *Appl. Opt.*, *24*(22), 3929–3932, doi:10.1364/AO.24.003929.

Winker, D. M., M. A. Vaughan, A. H. Omar, Y. Hu, K. A. Powell, Z. Liu, W. H. Hunt, and S. A. Young (2009), Overview of the CALIPSO mission and CALIOP data processing algorithms, *J. Atmos. Oceanic Technol.*, *26*, 2310–2323, doi:10.1175/2009JTECHA1281.1.

R. Ferrare and J. Hair, NASA Langley Research Center, MS 401A, Hampton, VA 23681, USA. (richard.a.ferrare@nasa.gov)

D. Giles and J. Schafer, SSAI, NASA Goddard Space Flight Center, Greenbelt, MD 20771, USA. (joel.schafer@nasa.gov)

C. Hostetler, NASA Langley Research Center, MS 420, Hampton, VA 23681, USA.

C. J. McPherson and J. A. Reagan, Department of Electrical and Computer Engineering, University of Arizona, 1230 E. Speedway Blvd., Tucson, AZ 85721, USA. (cjm3@email.arizona.edu)